

Zeitschrift: Eclogae Geologicae Helvetiae
Herausgeber: Schweizerische Geologische Gesellschaft
Band: 96 (2003)
Heft: 3

Artikel: High-resolution record of lateral facies variations on a shallow carbonate platform (Upper Oxfordian, Swiss Jura Mountains)
Autor: Samankassou, Elias / Strasser, André / Di Gioia, Eric
DOI: <https://doi.org/10.5169/seals-169030>

Nutzungsbedingungen

Die ETH-Bibliothek ist die Anbieterin der digitalisierten Zeitschriften auf E-Periodica. Sie besitzt keine Urheberrechte an den Zeitschriften und ist nicht verantwortlich für deren Inhalte. Die Rechte liegen in der Regel bei den Herausgebern beziehungsweise den externen Rechteinhabern. Das Veröffentlichen von Bildern in Print- und Online-Publikationen sowie auf Social Media-Kanälen oder Webseiten ist nur mit vorheriger Genehmigung der Rechteinhaber erlaubt. [Mehr erfahren](#)

Conditions d'utilisation

L'ETH Library est le fournisseur des revues numérisées. Elle ne détient aucun droit d'auteur sur les revues et n'est pas responsable de leur contenu. En règle générale, les droits sont détenus par les éditeurs ou les détenteurs de droits externes. La reproduction d'images dans des publications imprimées ou en ligne ainsi que sur des canaux de médias sociaux ou des sites web n'est autorisée qu'avec l'accord préalable des détenteurs des droits. [En savoir plus](#)

Terms of use

The ETH Library is the provider of the digitised journals. It does not own any copyrights to the journals and is not responsible for their content. The rights usually lie with the publishers or the external rights holders. Publishing images in print and online publications, as well as on social media channels or websites, is only permitted with the prior consent of the rights holders. [Find out more](#)

Download PDF: 12.07.2025

ETH-Bibliothek Zürich, E-Periodica, <https://www.e-periodica.ch>

High-resolution record of lateral facies variations on a shallow carbonate platform (Upper Oxfordian, Swiss Jura Mountains)

ELIAS SAMANKASSOU¹, ANDRÉ STRASSER¹, ERIC DI GIOIA¹, GAËTAN RAUBER¹ & CHRISTOPHE DUPRAZ²

Key words: Carbonate platform, facies analysis, sequence stratigraphy, cyclostratigraphy, Oxfordian

ABSTRACT

In the Upper Oxfordian Steinebach and Hauptmumienbank Members of the Swiss Jura Mountains, lateral and vertical facies changes are quantified. Five sections (Roderis, Chaltbrunnental I, Chaltbrunnental II, Les Champés, and Court) have been measured bed-by-bed and sampled in detail while also identifying sedimentary structures and lateral variations in thickness and facies.

A laterally continuous outcrop in the Roderis section reveals facies changes over very short distances: beds of ooid grainstones pass into thicker layers of coral rudstones, and coral reefs up to 1.5 m thick pinch out laterally within 10 to 20 m. The facies mosaic with its short-distance variations, both lateral and vertical, indicates a dynamic and complex sedimentary system where juxtaposed sub-environments evolved and shifted through time.

The sequence- and cyclostratigraphic interpretation of the studied sections allows for kilometer-scale correlation. In each section, elementary and small-scale depositional sequences can be identified, which correspond to the 20-ka orbital precession cycle and to the 100-ka eccentricity cycle, respectively. It is implied that ooid shoals were generally active in the transgressive parts of the small-scale sequences. Marly intervals including echinoderms, brachiopods, sponges, and ammonites accumulated around maximum-flooding surfaces. Coral patch-reefs flourished locally in highstand conditions. Sequence boundaries and maximum-flooding surfaces of the small-scale sequences correlate easily, indicating that their development was mainly controlled by a common, external factor. Deepening- and shallowing-trends in elementary and small-scale sequences imply that this factor was sea level. Facies varies also at a larger scale, due to differences in antecedent sea-floor morphology. Differential subsidence strongly influenced accommodation space within a short lateral distance (<10 km).

Our results show that one should be careful with long-distance correlations based on facies alone, particularly when dealing with shallow-water carbonate platform deposits where biostratigraphic control is limited.

ZUSAMMENFASSUNG

Laterale und vertikale Faziesänderungen in Sedimentabfolgen der Steinebach und Hauptmumienbank Members im oberen Oxford des Schweizer Jura wurden quantifiziert. Fünf Profile (Roderis, Chaltbrunnental I, Chaltbrunnental II, Les Champés und Court) wurden Bank-für-Bank gemessen und detailliert beprobt, unter Berücksichtigung der lateralen Variationen von Fazies und Mächtigkeiten.

Faziesänderungen im sehr kleinen Massstab sind im Aufschluss Roderis sichtbar, wo die Abfolge lateral gut verfolgt werden kann: Bänke aus Ooid-Grainstones gehen in dicke Lagen aus Korallen-Rudstones über, und 1.5 m dicke Korallenriffe keilen lateral innerhalb von 10 bis 20 m aus. Das Faziesmosaik auf kleinsten Raum, sowohl lateral als auch vertikal, zeigt dass es sich um ein dynamisches und komplexes sedimentäres System handelte, wo angrenzende Ablagerungsräume sich im Laufe der Zeit fortentwickelt und verschoben haben.

Durch die sequenz- und zyklusstratigraphische Interpretation konnten die untersuchten Profile im Kilometermassstab korreliert werden. In jedem Profil werden elementare und kleine Ablagerungssequenzen identifiziert, die dem orbitalen 20-ka Präzessions-Zyklus und dem 100-ka Exzentrizitäts-Zyklus entsprechen. Daraus ergibt sich, dass Ooidbarren im Allgemeinen während der transgressiven Phasen der Kleinsequenzen aktiv waren. Mergelige Intervalle mit Echinodermen, Brachiopoden, Schwämmen und Ammoniten kommen im Bereich der Flächen maximaler Überflutung vor. Fleckenriffe gedeihen lokal bei Hochständen des Meeresspiegels. Sequenzgrenzen und Flächen maximaler Überflutung der Kleinsequenzen korrelieren gut, was darauf hinweist, dass die Entwicklung auf einen gemeinsamen, externen Kontrollfaktor zurückzuführen ist. Vertiefungs- und Verflachungstendenzen in den Elementar- und Kleinsequenzen deuten auf Meeresspiegel als Kontrollfaktor hin. Die Fazies variiert auch im grösseren Massstab, diktiert durch die Morphologie des Meeresbodens. Differenzielle Subsidenz konnte den Akkommodationsraum über kurze Distanzen (<10 km) stark beeinflussen.

Unsere Ergebnisse zeigen, dass man vorsichtig sein muss mit weiträumigen Korrelationen, die allein auf Fazieskriterien basieren. Dies gilt vor allem für Flachwasserablagerungen auf Karbonatplattformen, wo die biostratigraphische Kontrolle beschränkt ist.

¹ Department of Geosciences, Geology-Palaeontology, University of Fribourg, Pérolles, CH-1700 Fribourg, Switzerland

² Institute of Geology, University of Neuchâtel, Rue Emile-Argand 11, CH-2700 Neuchâtel, Switzerland. E-mail: elias.samankassou@unifr.ch

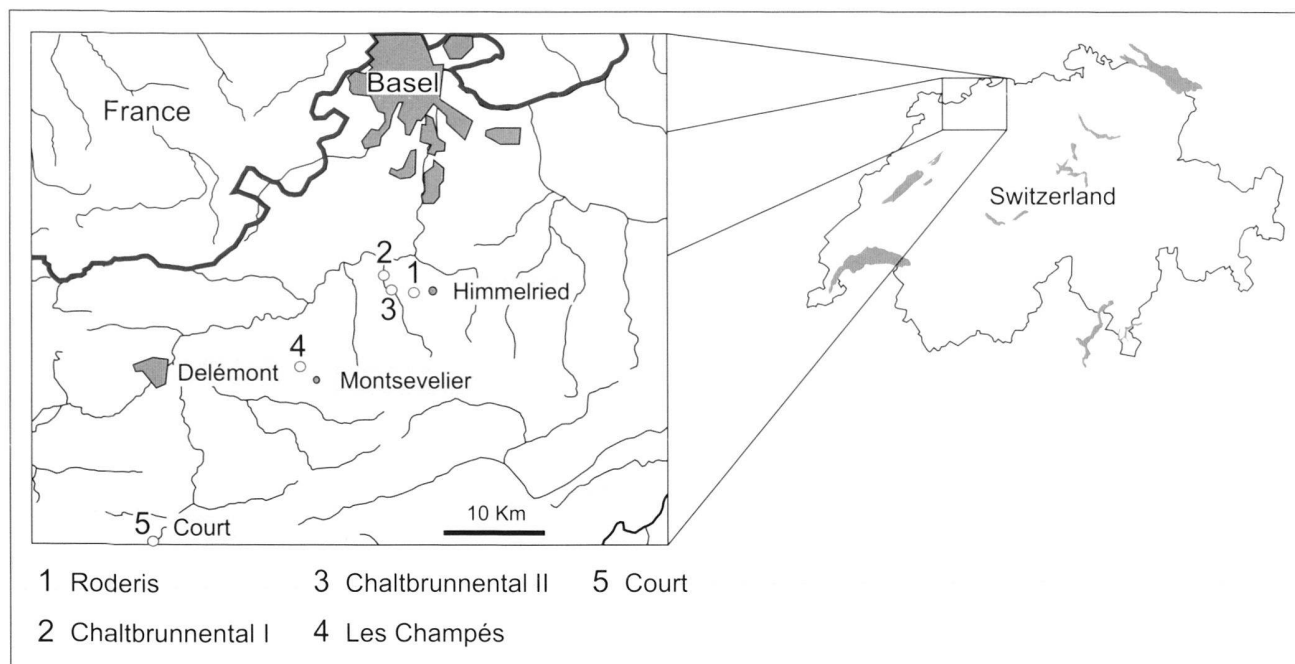


Fig. 1. Location of the study area and sections.

1 Introduction

Over the last years, sequence-stratigraphic and cyclostratigraphic studies in the Swiss and French Jura Mountains have resulted in high-resolution correlations of Upper Jurassic (Oxfordian and Kimmeridgian) shallow-water carbonate strata (e.g., Pittet 1996, Dupraz 1999, Colombié 2002). Within the biostratigraphic framework given by Gygi (1995) and based on the sequence-chronostratigraphic chart of Hardenbol et al. (1998), depositional sequences corresponding to the 20-, 100-, and 400-ka orbital cycles (Milankovitch cycles) could be identified. Thus, a very narrow time frame is available, within which facies evolution can be analysed and interpreted.

The database for our previous work stemmed mainly from densely sampled vertical sections in road-cuts, quarries, or mountain cliffs. The interpretation of facies changes through time then led to a hypothetical model of various juxtaposed depositional environments, from paleosols through tidal-flats and lagoons to patch-reefs and ooid shoals. Outcrop conditions generally did not allow for studying lateral facies variations in detail. This, however, is important if the functioning of an ancient carbonate platform is to be understood. Modern shallow-water carbonate systems display a multitude of co-existing sedimentary environments, and the controlling parameters are fairly well known (e.g., Enos & Perkins 1977, Scoffin 1987, Tucker & Wright 1990). With the time resolution of a few 10 ka obtained by cyclostratigraphy, the time range within which the ancient sediments can be studied is similar to that of the Holocene, and a comparison with their modern counterparts is thus facilitated.

In the present paper, we focus on closely spaced sections and on an outcrop that allows to follow individual depositional sequences over tens of metres. We show that lateral facies variations are important and even contribute to shaping the sea-floor morphology. Furthermore, we demonstrate that short gaps in the sedimentary record occur at regular intervals and are controlled by high-frequency, low-amplitude sea-level fluctuations.

2 Geographic setting, stratigraphy, and palaeogeography

The study area is located in the Swiss Jura Mountains, south of the town of Basel, Switzerland (Fig. 1). The Court and Les Champés sections are situated in the folded part of the Jura, while the Chaltbrunnental I and II sections and the one of Roderis lie in the tabular part of the Jura Mountains (Laubscher 1995).

The examined strata belong to the Steinebach and Hauptmumienbank Members in the Upper Oxfordian (Fig. 2; Gygi 1995). Some poorly preserved Perisphinctid fragments have been found in the Roderis section (Di Gioia 2001) but do not reveal any precise biostratigraphic information (pers. comm. R.A. Gygi). However, by lateral correlation, the two members can be placed in the Hypselum subzone of the Bimammatum zone (Fig. 2; Gygi & Persoz 1986, Gygi 1995). The on-coid-rich Hauptmumienbank ("main mummy bed") received its name from Ziegler (1956), who was inspired by Steinmann's (1880) comparison of microbially-wrapped grains with Egyptian mummies. The oolitic Steinebach Member has

		SB	Ammonite chrons	Ammonite sub-chrons	Formations	Canton Jura (West)	Canton Bern (Central)	Canton Solothurn (East)	
OXFORDIAN	Late	Ox8 154.6	Planula	Galar	Courgenay	Porrentruy Member	Formation	Verena Member	Holzflue Member
				Hauffianum		La May Member		Laufen Member	
		Ox7 155.2	Bimammatum	Bimammatum	Vellerat	Bure-Member	Hauptmumienbank Member	Steinebach Member	Olten Coral Limestone
				Hypselum					
	Middle	Ox6 155.8	Bifurcatus	Grossouvrei	St. Ursanne	Röschenz Member	Balsthal	Günsberg Member	Effingen Member
				Stenocycloides					
				Schilli					
		Ox5 157.0	Transversarium	Parandieri	St. Ursanne	Vorbourg Member	Wildegge Formation	Pichoux Formation	Birmenstorf Member
	Ox4 157.4	Antecedens		St. Ursanne Formation					

Fig. 2. Oxfordian stratigraphy of the northern Swiss Jura Mountains. The shaded field indicates the stratigraphic position of the interval studied in this paper. Litho- and biostratigraphy according to Gygi (1995, 2000), sequence boundaries (SB, e.g., Ox7) and their ages in Ma according to Hardenbol et al. (1998).

been introduced by Gygi (1969; originally “Steinibach Schicht”).

The studied members overlie marls with intercalated thin limestone beds of the Röschenz and Günsberg Members and are capped by reddish oolitic limestone of the Oolithe Rousse Member, or by bioclastic-oncolitic limestones of the Laufen Member (Fig. 2). In sequence-stratigraphic terms, the Steinebach and Hauptmumienbank Members constitute the transgressive and highstand systems tracts of a third-order sequence (Pittet 1996, Gygi et al. 1998, Hug 2003). The lower boundary of this sequence, labeled Ox6 by Hardenbol et al. (1998), is placed in the marly members below, the upper boundary Ox7 on the top of the studied members. Root traces and other plant material are common around these boundaries.

During Oxfordian times, the Jura was part of the northern margin of the Tethys ocean (Ziegler 1988). The palaeolatitude is estimated at 26 to 28 °N (Dercourt et al. 2000). Land areas to the north of the shallow, sub-tropical carbonate platform (such as the Bohemian and London-Brabant massifs; Ziegler 1988) periodically furnished siliciclastics.

3 Measured sections and methods

The Roderis section is located to the north of the village of that name, along the road leading from Nunningen to Grellingen (Swiss coordinates 611°820/251°180 to 611°890/251°400). In the Chaltbrunnental, a valley running more or less parallel to the above-mentioned road but 1 km to the west, two further sections were measured (609°750/252°750 and 610°930/251°250).

The Roderis section is 17 m, the Chaltbrunnental I and II are 24 m and 19 m thick, respectively. These three sections have been studied in detail by Di Gioia (2001). Special emphasis is given to the Roderis outcrop, due to its unique laterally continuous exposure.

The Les Champés section crops out along a forest road that leads into a small valley cutting through the anticline SSE of Bärschwil (603°680/246°560 to 603°460/246°380). This section was first published by Gygi (2000) with the label RG400, and was later studied in great detail by Rauber (2001). It starts in the Middle Oxfordian and ends in the Lower Kimmeridgian, but only the Hauptmumienbank Member will be discussed here.

The Court section follows the road leading from Moutier to Court, through the cut in the Graiterie anticline. It covers the Middle Oxfordian to Kimmeridgian and has been analysed in detail by Pittet (1996), Gygi (2000), Colombié (2002), and Hug (2003). The Steinebach Member and the base of the Hauptmumienbank Member have been studied on the northern flank of the anticline (593°310/234°470). The outcrop then becomes inaccessible, and the upper part of the Hauptmumienbank was sampled on the southern flank of the anticline (592°950/233°000).

The collected material in the studied interval consists of 135 samples. Polished slabs of each sample and 54 thin sections were analysed. The detailed petrographic analysis includes the qualitative determination of texture, non-carbonate minerals (quartz and pyrite), bioclasts, non-bioclastic grains, matrix, cements, and the evaluation of the relative abundances of these components (example in Fig. 3).

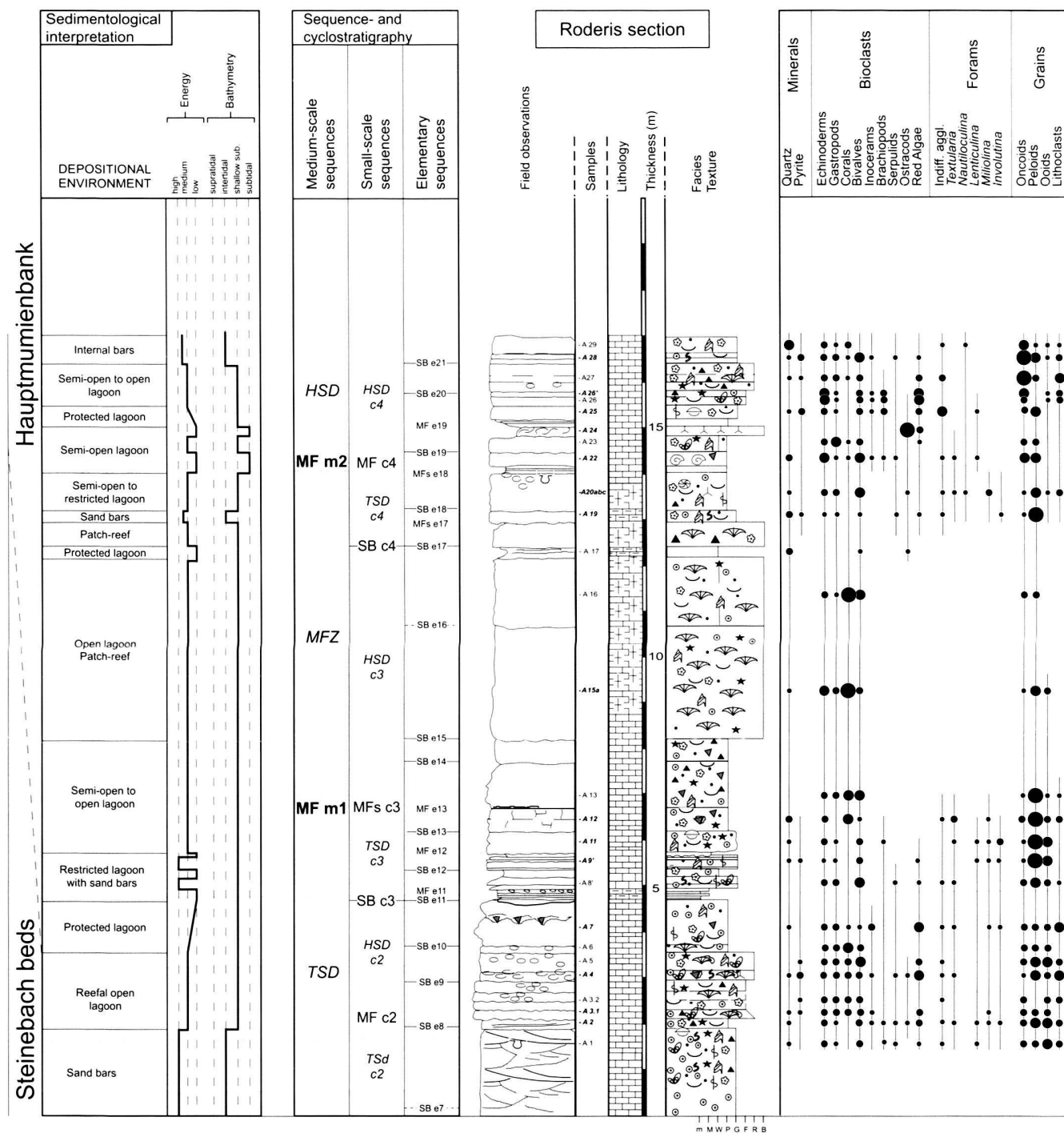


Fig. 3. Log of the Roderis section including lithology, facies, texture, relative abundance of components, as well as sedimentological, sequence- and cyclostratigraphic interpretations. SB = Sequence boundary; TSD = Transgressive deposits; MF = Maximum flooding (S: surface, Z: zone); HSD = Highstand deposits.

4 Facies analysis

Facies interpretation of sedimentary rocks is usually based on vertical sections, often assuming large-scale continuous facies belts, although meter-scale facies juxtaposition is well known

from modern and Holocene shallow-water depositional environments (e.g., Enos & Perkins, 1977). The detailed sampling and the microfacies analysis permit the definition of small-scale variations and help to interpret the interplay of physical



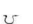

























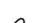



	Birdseyes		Ammonites
	Bioturbation		Bivalves
	Desiccation cracks		Brachiopods
	Lithoclasts		Bryozoans
	Nodules		Corals
	Oncoids		Encrusted corals
	Ooids		Coral fragments
	Peloids		Encrusted coral fragments
	Desiccation polygons		Echinoderms
	Serpulids		Sponges
	Stromatolites		Foraminifera
	Thalassinoides		Gastropods
	Red algae		Inoceramids
	Green algae		Ostracodes
	Charophytes	m	Marls
	Dasycladacean algae	M	Mudstone
	Plant debris	W	Wackestone
	Roots	P	Packstone
		G	Grainstone
		F	Floatstone
		R	Rudstone
		B	Boundstone

Fig. 3. continued

and ecological parameters during deposition. The facies analysis follows the classification scheme of Dunham (1962) and Embry & Klovan (1972). We recognize seven main microfacies types, which are briefly described and interpreted below.

4.1 Floatstones

Allochems consist of sub-angular, large (up to 10 cm in diameter) coral debris, various bioclasts (including the red alga *Solenopora*, echinoderms, and bivalves), and lithoclasts (0.2 – 4 cm in diameter). Boring of bioclasts is widespread, particularly in the Les Champés section. The matrix consists of wackestones containing abraded bioclasts.

The large debris indicate the proximity to a high-energy environment. However, there are no sedimentary structures indicative of storm influence (e.g., layers of tempestites). The association of corals, red algae, and echinoderms indicates

open-marine conditions. The environment was therefore probably located close to an open platform margin or bar.

4.2 Rudstones

Two sub-types can be differentiated among the rudstone facies according to its components.

- (1) Rudstone with ooids: Cross-bedding and herring-bone structures are characteristic of this facies (Figs. 3 and 4). Grains are well sorted. Large ooids (pisoids according to some authors, as the diameter exceeds 2 mm; see Flügel 1982 for discussion) occur, along with the benthic foraminifera *Nautiloculina* sp. and *Lenticulina* sp. Patches of micrite fill parts of the interparticle porosity. Sandwaves and the abundance of ooids indicate a high-energy, probably tidally influenced environment, and allow the interpretation of the depositional environment as winnowed carbonate shoals or tidal bars (Flügel 1982). The shoals or bars may have temporarily been abandoned, enabling deposition of mud. Alternatively, they may have been colonized and mud may have then been trapped, in analogy to the Recent shoals of the Bahamas (Neumann et al. 1970, Scoffin 1970).
- (2) Rudstone of reef debris: Large, sub-angular, poorly sorted debris of strongly recrystallized massive and branched corals account for more than 70% of the total components in this facies. Recognizable corals are *Stylina* sp. and *Helio-coenia variabilis* (regrouped into the family 'Stylinids' sensu Gill, 1977), the phaceloid *Calamophylliopsis* sp., ramoses *Thamnasteria* sp., and actinacidids, probably *Actinarae* sp. (Fig. 5). Further fossils include gastropods, bivalves, the sponge *Cladocoropsis mirabilis*, and miliolid foraminifera.

The depositional environment was probably located close to coral patch reefs (see below), from which most of the debris was derived. The proximity to coral patch reefs is deduced from the poor sorting and angular forms of the coral debris, and the similarity of the latter to corals of the boundstone facies, in analogy to the facies surrounding most of modern lagoonal patch reefs (e.g., Jordan 1973, James & Ginsburg 1979).

4.3 Packstones and grainstones

Three sub-facies are recognized within the packstone and grainstone facies.

- (1) Cross-bedded layers consisting of ooids, oncoids, and benthic foraminifera as main components. Radial, superficial, and micritic ooids are encountered (Fig. 6A, B). Neomorphic sparite and dolomite occur in a few thin sections. The presence of micrite indicates phases of lowered energy, during which high-energy bars were temporarily abandoned. The occurrence of different ooid types indicates

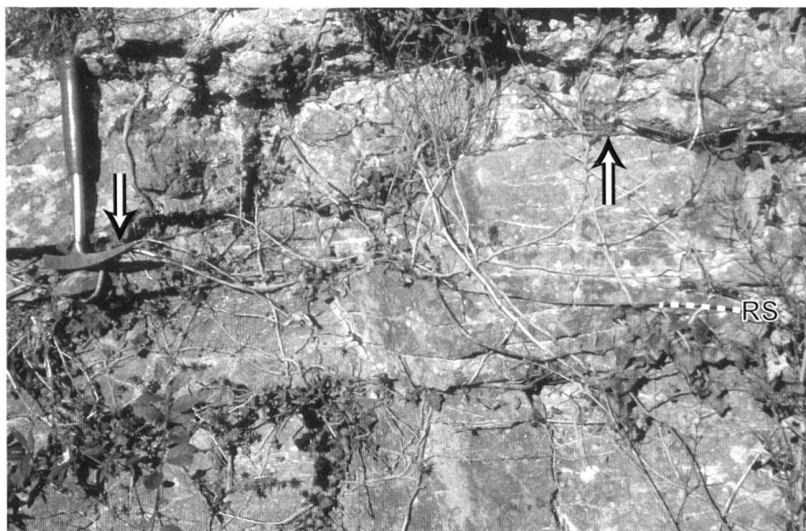


Fig. 4. Oolitic sand waves from the basal part of the Roderis section. Note the small-scale relief (arrows) and the high angles of the reactivation surfaces (RS). Hammer is 32 cm long.

varying conditions during deposition, e.g., in energy and/or salinity (Flügel 1982, Strasser 1986).

- (2) Packstone and grainstone with diverse fossils including brachiopods, echinoderms, bivalves (*Inocerams*), gastropods (*Nerinea* sp.), benthic foraminifera (*Lenticulina* sp., *Cyclamminids*), algae, ammonites (one specimen), and problematic fossils (*Tubiphytes*, *Lithocodium*). Oncoids are common. The high-diversity biota indicate open-marine conditions.
- (3) Packstone and grainstone with low-diversity fossils including bivalves, the gastropod *Nerinea* sp., and benthic agglutinated foraminifera are characteristic of this subfacies. Ostracodes are very common in distinct layers. Peloids and ooids are common. Detrital quartz occurs, and reaches 30% in some thin sections. The low-diversity biota, along with the dominance of ostracodes, imply restricted conditions during deposition.

The overall features of this facies indicate a lagoonal depositional environment. A similar facies, including a normal-marine fauna interpreted as resulting from good circulation and exchange with the open sea through tidal inlets in the barrier, is reported from the mid-Jurassic Lincoln Limestone Formation, England (Tucker 1985). There, a more inshore low-energy zone and higher energy outer lagoon are differentiated. However, for the studied system, the existence of barrier-islands can only be inferred (Hug 2003). Skeletal-peloidal sands and lime mud are typical of lagoonal facies (e.g., Trucial Coast, Arabian Gulf; Purser 1973, Schreiber 1986).

4.4 Coral boundstone

Isolated carbonate bodies composed of massive and branching corals mostly in growth position occur in the Roderis section (Fig. 5C). The flanks of these bodies consist of rudstone (see

description above). We distinguish four coral growth forms: ramose corals (*Thamnasteria* sp.), 30–40 cm high (Fig. 5C, D); phaceloid corals (*Calamophylloids* sp.), 15–20 cm high (Fig. 5B, E, F); flat, sheet-like corals (strongly recrystallized *Actinacidae*, probably *Actinariae* sp.), approximately 10 cm thick and up to 1 m wide (Fig. 5F, I); and globular, head-like corals (stylinids sensu Gill, 1977) up to 10 cm in diameter (Fig. 5G, H). Boundstone is the characteristic microfacies. The matrix consists of peloidal packstone and grainstone. Echinoderms and bivalves are common. Encrustations by microbialite, foraminifera (Fig. 6C), *Terebella* worms, or bryozoans as well as borings (*Gastrochaenolites*) are widespread (Fig. 6D). Commonly, flat corals are found in the basal part of the bioherms, followed upward by massive forms, and dendroid types at the top.

The occurrence of isolated, individual buildups points to coral patches similar to today's lagoonal patch reefs such as those within the system of the Great Barrier Reef in Australia (Scoffin 1987) or off Bermuda (Garret et al. 1971). Rudstone on the flanks of the buildups and the matrix of packstone and grainstone indicate high-energy conditions, or the presence of channels between individual buildups where coarse material accumulated. The high diversity of fossils indicates overall open-marine conditions.

The vertical zonation observed in several buildups is striking: flat and massive corals (Fig. 5) in the lower part of the buildups and branched forms at the top. Such a coral zonation typically indicates a deepening-upward trend (James & Bourque 1992). Furthermore, marls including ammonites occur above the uppermost sequence in the Roderis section (Fig. 3).

4.5 *Tubiphytes* boundstone

This facies is generally associated with the coral boundstone. *Tubiphytes* forms an intertwined framework, surrounded by

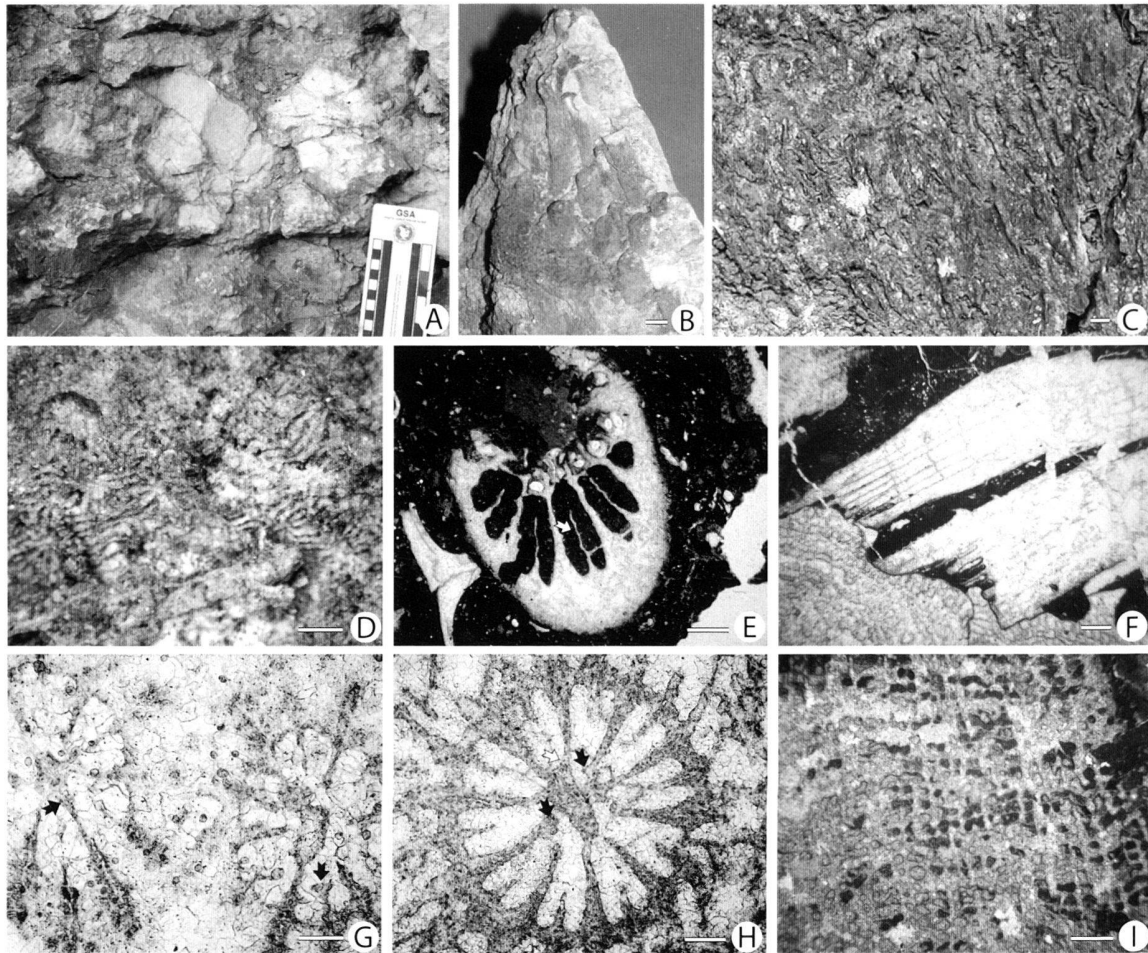


Fig. 5. Rudstone and framestone facies of the Roderis section.

- A. Rudstone facies showing large debris of massive corals (Stylinids and Actinaricids). Outcrop picture.
 B. *Calamophylliopsis* sp. Macroscopic view (sample RCD 3), scale bar 5 mm long.
 C. Ramose *Thamnasteria* sp. Outcrop picture, scale bar 5 mm long.
 D. Surface of *Thamnasteria* sp., oblique section. Binocular lens (sample RCD 5), scale bar 1 mm long.
 E. *Calamophylliopsis* sp., transversal section. Note the typical 'zigzag' shaped septum (white arrow). Thin section RCD 2, scale bar 500 µm long.
 F. *Calamophylliopsis* sp., longitudinal section, close to an actinacidid coral. Thin section RCD 2, scale bar 1 mm long.
 G. *Styliina* sp., transversal section. Note the developed auricles (black arrows; Gill, 1977). Thin section RCD 1, scale bar 500 µm long.
 H. *Heliocoenia* sp., transversal section. Also note the auricles (black arrows) and the attachment to the columella (white arrow). Thin section RCD 5, scale bar 500 µm long.
 I. Partly recrystallized actinacidid corals, probably *Actinaraea* sp., longitudinal section. Thin section RCD 3, scale bar 500 µm long.

and including at least three micritic crusts (Fig. 6E). The remaining matrix is wackestone. Sessile foraminifera constitute the sparse remaining fossils within the *Tubiphytes* boundstone.

This facies is indicative of a tranquil, sheltered setting between coral colonies. *Tubiphytes* seems to exclude other biota, as indicated by the scarce associated fossils. The low diversity of biota might result from ecological conditions in the sheltered settings (e.g., limited water circulation, reduced light; Dupraz & Strasser 1999, 2002).

4.6 Wackestone

The wackestone facies exhibits a low-diversity fossil association consisting of a few bivalves, gastropods, agglutinated foraminifera, and ostracodes. The rocks are partly bioturbated. Dolomitization is widespread. Clotted micrite is abundant in some samples.

The low-diversity biota point to restricted marine conditions during deposition. The local presence of evaporites may indicate times of limited water circulation and supratidal conditions that permitted evaporation. The clotted fabrics point to microbial activity in the carbonate mud (e.g., Reitner et al. 1995).

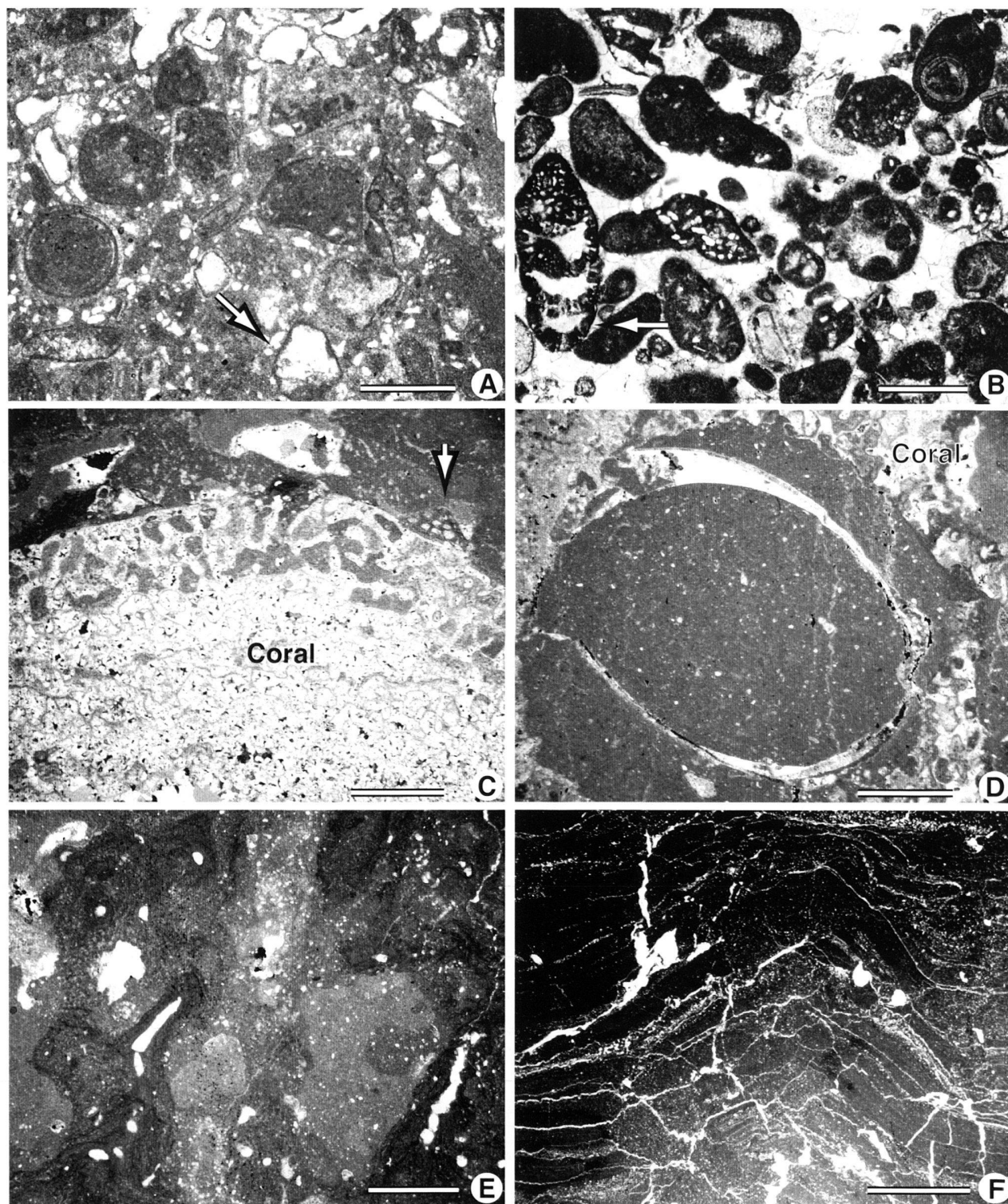


Fig. 6. A. Ooid-bioclack packstone. Note the micritic envelopes around dissolved bioclacks, suggesting lagoonal conditions. Scale bar is 1 mm long.
 B. Grainstone. Components include coated grains (ooids and oncoids), dasycladaceans, and foraminifera (arrow: *Pseudocyclammina* sp.). Scale bar is 1 mm long.
 C. Detail of a coral skeleton overgrown by a foraminifer (arrow). Scale bar is 0.5 mm long.
 D. Boring bivalve in a coral skeleton. Mud filled the residual space. Scale bar is 1 mm long.
 E. *Tubiphytes* boundstone. The matrix consists of micritic crusts and unfossiliferous mudstone. Scale bar is 0.5 mm long.
 F. Laminated mudstone. Note tepee-like structure and the multiple fenestrae. Scale bar is 4 mm long.

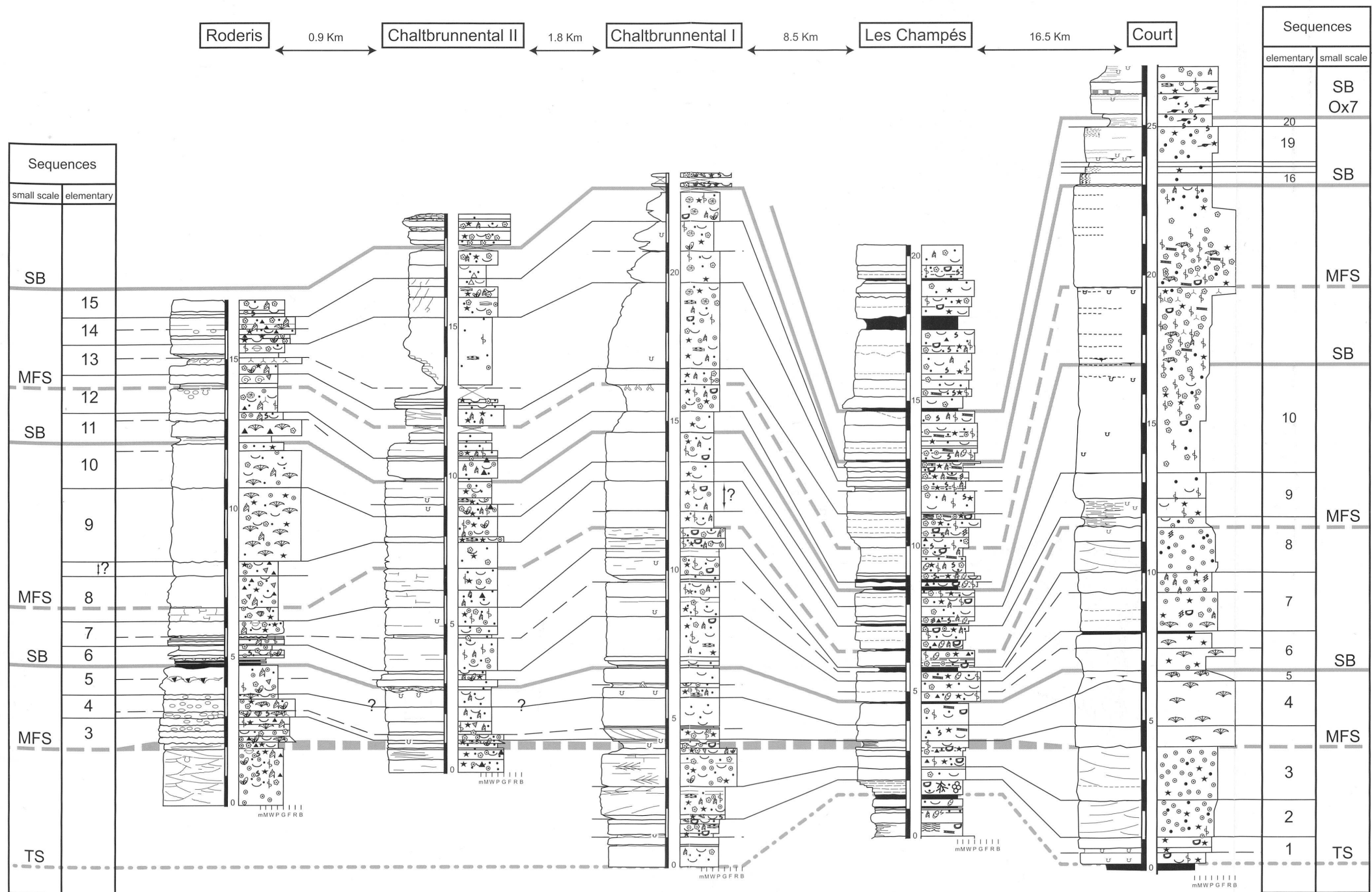


Fig. 7. Best-fit correlation of the studied sections based on the sequence- and cyclostratigraphic correlation discussed in the text. For symbols refer to Fig. 3. SB: Sequence boundary; TS: transgressive surface; MFS: Maximum-flooding surface; Ox7: Oxfordian sequence boundary 7 according to Hardenbol et al. (1998)

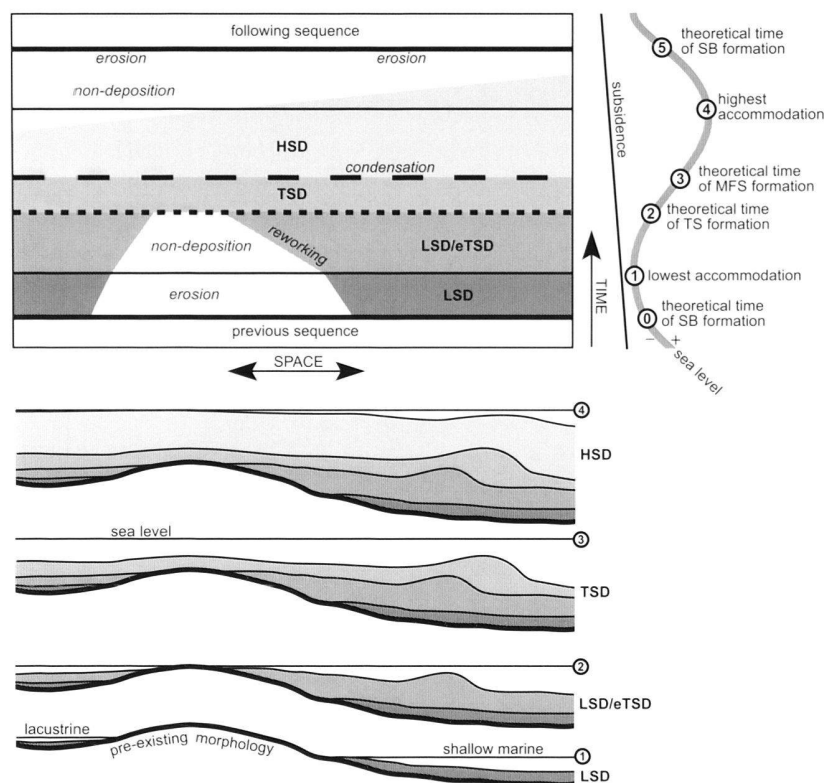


Fig. 8. Distribution of sediment through time as a function of sea-level change (one 20-ka cycle) and basin morphology. Sedimentation rates vary according to position on the transect. Note that different depositional environments are juxtaposed preferentially during lowstand and early transgressive conditions, while a homogenization potentially occurs during maximum flooding. SB: sequence boundary; TS: transgressive surface; MFS: maximum-flooding surface; LSD: lowstand deposits; TSD: transgressive deposits; eTSD: early transgressive deposits; HSD: highstand deposits.

4.7 Mudstone

Mudstone is usually laminated and may also exhibit bioturbation, desiccation features, laminoid fenestrae, and tepee structures (Fig. 6F). Intraclasts commonly are of mudstone texture. The rare biota consist of miliolid and agglutinated foraminifera, and charophytes (Rauber 2001). Occasional root traces were also found.

The bioturbated, poorly fossiliferous mudstone with desiccation cracks, and the occurrence of intraclasts typically characterize a tidal flat (Shinn et al. 1969, Shinn 1983, Pratt et al. 1992). The presence of roots, tepee structures, and laminoid fenestrae points to long subaerial exposure periods (Ginsburg et al. 1977).

5 Sequence-stratigraphic interpretation

Based on the detailed analysis of facies, sedimentary structures, and bedding surfaces, each section is interpreted in terms of sequence stratigraphy (Figs 3 and 7). The sequence-stratigraphic terminology is that defined by Vail et al. (1991). In the studied sections, it is seen that the sedimentary record comprises three orders of depositional sequences: elementary, small-scale, and medium-scale sequences.

An *elementary sequence* is defined by a vertical facies evolution that translates one cycle of environmental change, in-

cluding sea-level change (Strasser et al. 1999). These sequences measure a few tens of centimetres to a few metres and are composed of one or several beds. The bedding planes are underlined by clay seams. Clays can be washed into the sedimentary system during a sea-level lowstand, and such a bedding plane would consequently be interpreted as a sequence boundary. However, clays can also be concentrated during maximum flooding when water energy decreases on the sea floor. Furthermore, increased rainfall in the hinterland can mobilize clays at any time of a sea-level cycle (Strasser & Hillgärtner 1998). The definition of an elementary sequence must therefore rely not only on bedding planes but also on the facies evolution (deepening-shallowing trends or more marine versus more restricted fossil assemblages). Where facies contrasts are not developed, or where autocyclical processes predominate, it might not be possible to identify elementary sequences.

Small-scale sequences measure a few metres in thickness and are generally composed of five elementary sequences (where these can be distinguished; Fig. 7). They display well-developed deepening-shallowing trends. The sequence boundaries are locally underlined by erosion surfaces. The following lowstand to early-transgressive deposits may contain reworked pebbles and, as in the Les Champés section, charophytes. Transgressive deposits typically contain high-energy ooid facies, implying a deepening of the depositional environment and the influence of tidal currents. In the Court section, coral

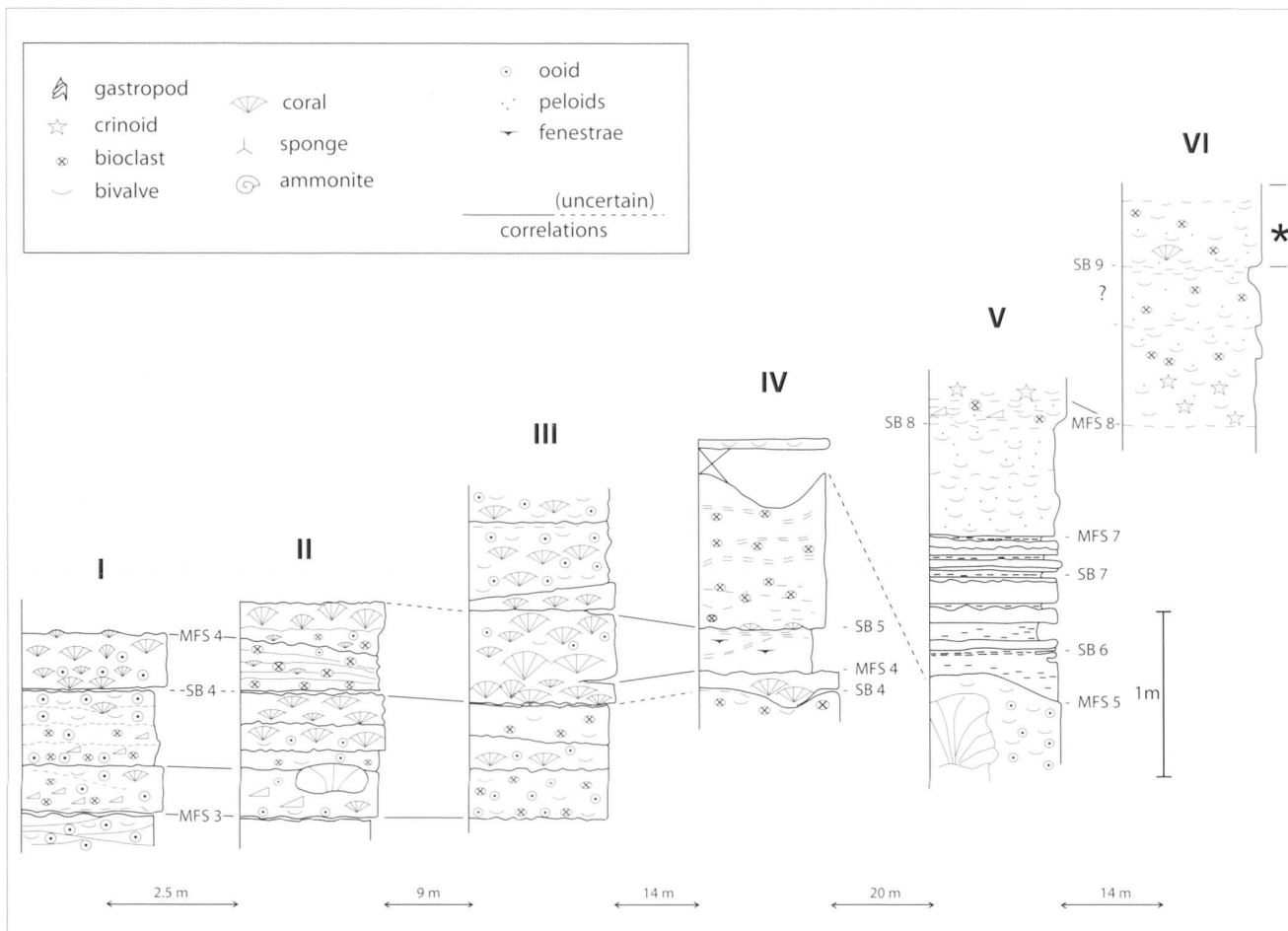


Fig. 9. Correlation of closely spaced sections along the road north of Roderis. Compare with Fig. 3, which shows the composite section. For discussion refer to text.

reefs also occur in a transgressive interval. Maximum flooding deposits are characterised by open-marine fauna, the relatively thickest beds pointing to highest accommodation, increased bioturbation suggesting reduced sedimentation rates, and an increased clay fraction leading to marly limestones. Highstand deposits of small-scale sequences commonly are dominated by lagoonal facies but may also contain coral reefs (in Roderis and Court).

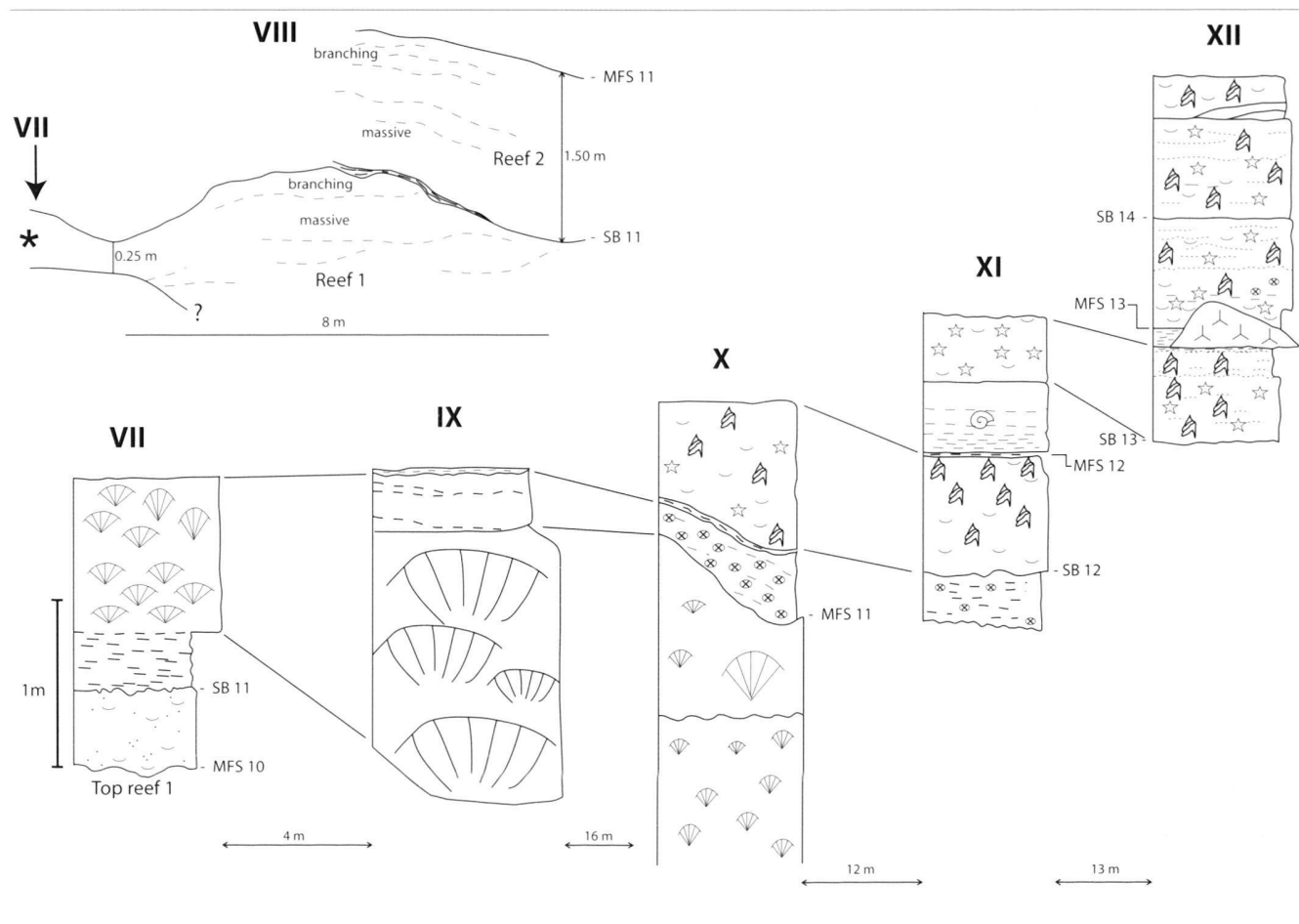
Medium-scale sequences cannot be demonstrated in the sections as represented in Figure 7 but become apparent when the sections are studied in their entirety (Raubert 2001; Hug 2003). Such sequences are composed of four small-scale sequences and show a general deepening-shallowing trend.

Once the analysis of the stacking pattern has been performed for each section, a correlation between the sections is attempted (Fig. 7). The sequence boundaries and maximum-flooding surfaces of the small-scale sequences correlate easily, whereas some question marks persist on the level of the elementary sequences. This may be due to a wrong interpretation

of some elementary sequences, or to autocyclical processes such as progradation or lateral migration of sedimentary bodies that simulate sequences (Strasser 1991). Nevertheless, the fact that most sequences can be correlated between the studied sections suggests that their development was controlled by a common factor. Deepening-shallowing trends in elementary, small-scale, and medium-scale sequences further imply that this factor was sea level, whereby at least three orders of sea-level fluctuations were superimposed.

The differences in thickness of the correlated sequences are partly explained by differential subsidence between the studied sections. However, also differential compaction may have played a role (Strasser et al. 2003). For example, the reefal boundstones composing elementary sequences 9 and 10 in Roderis certainly suffered less compaction than the lagoonal wackestones of the correlated sequences in Chaltbrunnental I and II (Fig. 7).

The Court section, of which only a part is shown in Figure 7, has been correlated with other shallow-water sections in the Swiss Jura and also with biostratigraphically well-dated deep-



er-water sections in the Swabian Alb (Gygi & Persoz 1986, Pittet 1996, Strasser et al. 2000, Hug 2003). The transgressive surface at the base of the sections shown in Figure 7 can be recognized throughout most of the Swiss Jura. It defines the limit between the marly top of the Röschenz and Günsberg Members and the limestones of the Steinebach respectively Hauptmumienbank beds.

The maximum-flooding surface of the second small-scale sequence (within elementary sequence 8) correlates with a condensed section in the Swabian Jura, situated between the Semimammatum and Berrense ammonite subzones (Schweigert 1995, Strasser et al. 2000). According to the sequence-chronostratigraphic chart of Hardenbol et al. (1998), this condensed section is dated at 155.4 Ma. The sequence boundary at the top of the Court section as represented in Figure 7 has been identified as the equivalent of sequence boundary Ox7 of Hardenbol et al. (1998) (Gygi et al. 1998, Strasser et al. 2000). It is situated below the reddish Oolithe Rousse Member (Gygi et al. 1998) and is dated at 155.2 Ma (Hardenbol et

al. 1998). The apparent precision of these dates is an artefact of interpolation, because only the stage boundaries are dated radiometrically. Furthermore, these include large margins of error (Callovia-Oxfordian 159 ± 3.6 Ma, Oxfordian-Kimmeridgian 154.1 ± 3.2 Ma; Gradstein et al. 1995). Nevertheless, these dates give a rough estimation of time comprised in the depositional sequences.

Detailed sequence-stratigraphic and cyclostratigraphic analyses of other Upper Oxfordian sections in the Swiss Jura have demonstrated that the small-scale sequences correspond to the first eccentricity cycle of the Earth's orbit (100 ka), and the medium-scale sequences to the second eccentricity cycle of 400 ka (Pittet 1996, Pittet & Strasser 1998, Strasser et al. 2000, Hug 2003). The fact that each small-scale sequence is commonly composed of 5 elementary sequences further implies that the latter formed in tune with the precession cycle of 20 ka (Berger et al. 1989). Between the maximum-flooding surface within elementary sequence 8 and sequence boundary Ox7 lie 12.5 elementary sequences. According to Hardenbol et al.

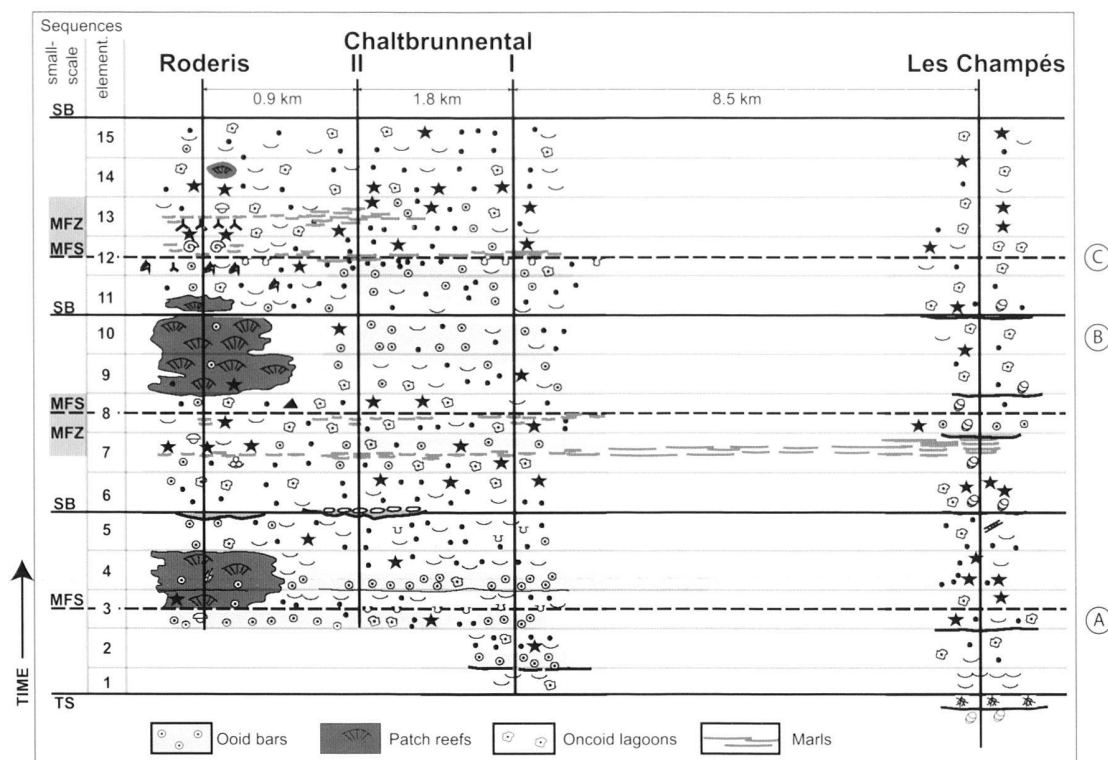


Fig. 10. Time-space diagram resulting from the sequence- and cyclostratigraphic interpretation. Hiatuses and condensation occurring on the scale of the elementary sequences are not shown. Between the closely spaced sections, major facies are interpolated. For discussion refer to text. Symbols as in Fig. 3.

(1998), this time interval covers 200 ka; according to our cyclostratigraphical interpretation it represents 250 ka.

Within the framework given by the correlations of sequence boundaries and maximum-flooding surfaces on the level of the elementary and small-scale sequences, lateral and vertical facies changes can now be traced and interpreted. Based on the hypothesis that an elementary sequence lasted 20 ka, a time frame for such changes can be determined.

If high-frequency sea-level cycles controlled the formation of the observed depositional sequences, then the formation of sequence boundaries and maximum-flooding surfaces can be assumed to be isochronous over the study area. However, the distribution of sediment within this time interval may be strongly diachronous and include hiatuses and condensation intervals (Fig. 8; Wheeler 1964). Sea-floor morphology, subsidence pulses, water energy, and the ecology of the carbonate-producing organisms may all have an influence on this distribution of sediment within a sequence.

6 Lateral and vertical facies changes

6.1 Metre-scale lateral variations

The Roderis outcrop shows remarkable short-distance, metre-scale lateral facies changes (Fig. 9). Beds composed of

ooid grainstone pass within 2 to 3 m into coral rudstone and boundstone (Fig. 9A, between I and II). A coral reef is juxtaposed to a level with birdseyes over a distance of only 14 m (Fig. 9A, III versus IV). This may have resulted from a short-term sea-level fall, recording the sequence boundary between elementary sequences 4 and 5. This sea-level fall led to an interruption of the reef growth, but not to its final subaerial exposure and death. A similar case is observed in section VIII (Fig. 9B). There, two successive reefs exhibit the same internal composition. The interruption corresponds to the sequence boundary between the elementary sequences 10 and 11. Coral reef bodies up to 1.5 m thick pinch out within 10 to 20 m distance (Fig. 9, between III and IV, and within VIII). This reflects the distribution of patch reefs within a shallow lagoon. Reefs expanded and coalesced as suggested by the geometries illustrated in VIII (Fig. 9B). The fossil content of some beds may also vary: e.g., a *Nerinea*-rich bed is continuous at one level (Fig. 9B, X through XI), whereas the crinoid-dominated bed in section XI passes into a *Nerinea*-dominated bed in section XII (Fig. 9B). The *Nerinea*-rich layers above the sponge bioherm (Fig. 9B, XII) show poor bedding. As seen in figure 10, these layers are within the maximum-flooding zone, where low-amplitude sea-level fluctuations did not lead to well-marked bedding. The bedding in the maximum-flooding interval around elementary sequences 7 and 8 is

even more difficult to define (V and VI, Fig. 9A). Overall, we found that reefs occur preferentially in highstand systems tracts of 100-ka cycles.

The occurrence of stacked coral reef bodies, each showing a characteristic vertical evolution from flat and massive to branching growth forms (Fig. 9B, VIII), points to longer-term sea-level rise creating accommodation space, on which shorter-term sea-level drops were superimposed. The sequence- and cyclostratigraphical analysis (see above) suggests that the major break between the two reef bodies in section VII was caused by a sea-level drop on the 100-ka scale. The reddish color of the marls underlining this break may result from sub-aerial exposure.

6.2. Kilometre-scale facies variations

To illustrate the lateral and vertical facies variations within the time frame established by sequence- and cyclostratigraphy, a time-space diagram has been drafted (Fig. 10). The dominant facies of each elementary sequence are placed in the corresponding time interval and interpolated between the closely-spaced sections of Roderis, Chaltbrunnental I, and Chaltbrunnental II. For simplicity, the hiatuses and condensed intervals that occur to various degrees in the elementary sequences are not represented (for the concept refer to Fig. 8).

The Roderis section displays the relatively most open-marine facies. Coral patch reefs flourished in highstand conditions of 100-ka cycles. The first reef complex lived for about 150 ka, the second one for 200 ka. Echinoderms, brachiopods, sponges, and ammonites accumulated preferentially around maximum-flooding surfaces. The sequence boundaries terminating the first two small-scale sequences suggest erosion and possibly subaerial conditions. Accommodation space must have been filled rapidly under good conditions for carbonate production, and the sea-level drop at the end of these sequences exposed the lagoon floor in elementary sequence 5 and the reef top in elementary sequence 10.

The two Chaltbrunnental sections are dominated by lagoonal facies rich in oncoids. Maximum-flooding conditions are indicated by increased bioturbation. Ooid shoals were active in the transgressive part of the first small-scale sequence during about 150 ka, coeval to the ones in Roderis. Later in the depositional history, ooids were washed in from nearby shoals and accumulated on the low-energy lagoon floor. Packstones and grainstones indicating high-energy conditions formed only sporadically and mainly during maximum-flooding conditions. This may indicate that barriers isolating the Chaltbrunnental lagoons from the open ocean were flooded during the fastest sea-level rise, thus admitting waves and currents to influence the lagoon. The top of the first small-scale sequence is eroded in Chaltbrunnental II, as is also the case in Roderis. However, the sea-level fall exposing the second reef in Roderis (top of elementary sequence 10) did not affect the lagoon-floor in the Chaltbrunnental sections, suggesting that the reef formed a positive relief at that time.

The Les Champés section is particular in that its sequences are relatively thin and its facies more restricted when compared to the other three sections (Figs 7 and 10). This implies that accommodation generally was low. Freshwater lakes with charophytes formed during sea-level lowstands or during early transgression, while maximum flooding allowed for establishment of lagoonal conditions with oncoids and normal-marine fauna. High-energy events frequently mixed freshwater and open-marine fauna and flora. Below the transgressive surface forming the base of the Steinebach Member (base of elementary sequence 1), freshwater facies are found in several successive elementary sequences. Within the Steinebach Member, however, the limestone beds of the elementary sequences containing charophytes also contain marine organisms. This implies that freshwater conditions reigned only during the lowstand, early-transgressive, and possibly late-highstand phases of a 20-ka sea-level cycle, whereas marine conditions were recorded around its maximum-flooding phase.

An interesting situation occurs around the maximum-flooding interval of the second small-scale sequence in Les Champés (within elementary sequences 7 and 8): charophytes are still common albeit mixed with marine fauna. This is explained by the sea-level drops related to the 20-ka orbital cycles that were sufficient to create fresh-water lakes in Les Champés, while conditions stayed subtidal in Roderis and in Chaltbrunnental. Climatically controlled eustatic sea-level changes certainly were synchronous on the Jura platform. Consequently, the Les Champés section must have formed on a topographic high with relatively low subsidence, while the other three sections experienced higher subsidence rates. Differential subsidence in the Swiss Jura has been demonstrated by, e.g., Pittet (1996) and Allenbach (2001). Furthermore, Allenbach (in press) proposed a synsedimentary fault passing between the Roderis/Chaltbrunnental area and Les Champés.

Three episodes have been chosen to illustrate the lateral facies variability (Figs 10 and 11). In the first time-slice (A in Figs 10 and 11), oolitic dunes composed of grainstone in the Roderis section are coeval to peloidal, bioturbated packstones and grainstones in both Chaltbrunnental sections. In the Les Champés section, the equivalent level is composed of peloidal wackestones and packstone including oncoids, echinoderms, and bivalves.

In the second episode (B in Figs 10 and 11), the coral framestone in the Roderis section is equivalent to peloidal-oolidal packstones and wackestones in the Chaltbrunnental sections. The same level in the Les Champés section consists of oncoid wackestones.

The third episode (C in Figs 10 and 11) is characterized by marly wackestones and packstone containing ammonites and sponges in the Roderis section, which correlates with open-lagoonal grainstones and packstones containing peloids, ooids, and oncoids in the Chaltbrunnental sections. The corresponding level in the Court section (Fig. 7) and in the Les Champés section is composed of open-lagoonal peloidal-oncoidal packstones to boundstones.

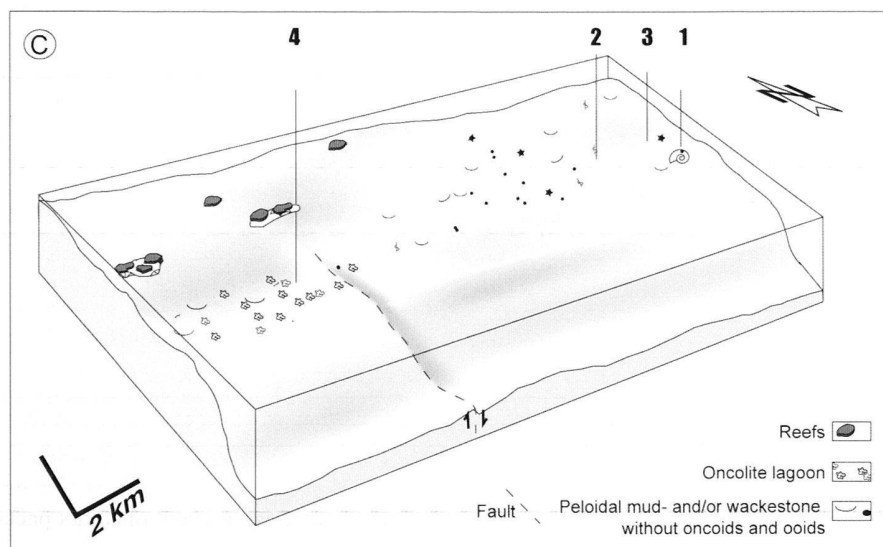
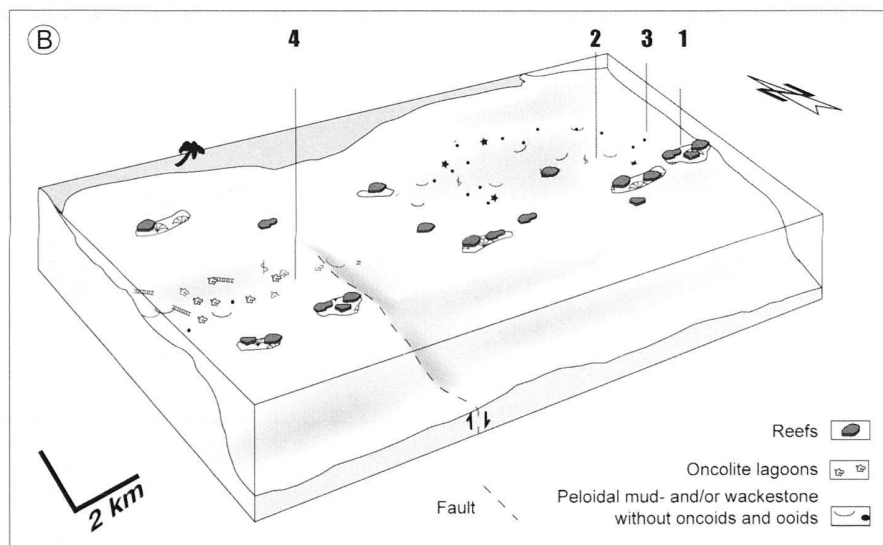
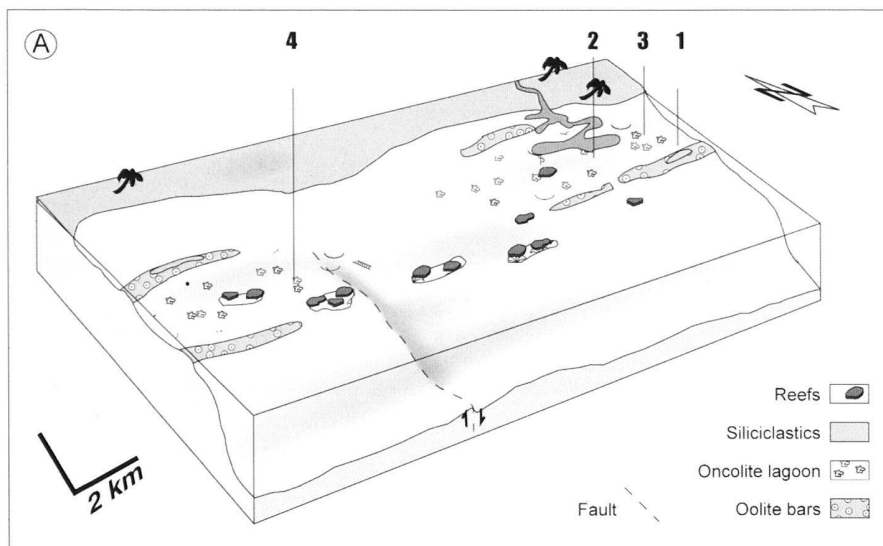


Fig. 11. Sketches of sea-floor at selected time intervals A, B, and C, as indicated in Fig. 10. The fault is inferred to explain the generally lower subsidence in the Les Champ  s section (4) when compared to Roderis (1), Chaltbrunnental I (2), and Chaltbrunnental II (3).

8 Conclusions

The lateral measurement of the Roderis section reveals metre-scale short-distance facies changes. Transition from ooid grainstone to coral rudstone occurs within a few metres. Intervals including birdseyes correlate with growth interruptions in reefs ca. 14 m away. Although vertical zonation in coral reef bodies points to long-term sea-level rise, the facies mosaic indicates a differentiated, non-uniform metre-scale sedimentary record. Short-distance facies variations, both lateral and vertical, indicate a dynamic and complex sedimentary system where juxtaposed sub-environments evolved and shifted through time.

The sequence- and cyclostratigraphic correlation as well as the time-space relationships reveal kilometre-scale variations in the evolution of the sedimentary environment. As sequence boundaries and maximum flooding surfaces of small-scale sequences correlate easily, a common, external factor to the development of facies can be assumed. Deepening- and shallowing-trends in elementary, small-scale, and medium-scale sequences imply that this factor was sea level. Overall, ooid shoals predominated during the transgressive parts of small-scale sequences, whereas marly layers including echinoderms, brachiopods, sponges, and ammonites characterized maximum flooding surfaces. Coral growth was important during high-stand conditions of 100-ka cycles.

Differences in antecedent topography and local tectonics were an additional control on accommodation. Furthermore, differential compaction contributed to differences in measured thickness. These results show that one should be careful with long-distance correlations based on facies alone. As biostratigraphic control is limited for shallow-water carbonate platform deposits, sequence- and cyclostratigraphy are shown as powerful tools for high-resolution correlation. A platform is a non-steady dynamic system that hardly can be subdivided into lateral facies belts consistent through time.

Acknowledgements

We thank Dr. R.A. Gygi for the determination of the ammonite from the Roderis section. The funding through grants of the Swiss National Science Foundation (Projects No. 20-56491.99 and 20-67736.02) is gratefully acknowledged. The journal referees A.C. Azerêdo and R.P. Allenbach are thanked for their constructive reviews.

REFERENCES

- ALLENBACH, R.P. 2001: Synsedimentary tectonics in an epicontinental sea: a new interpretation of the Oxfordian basins of northern Switzerland. *Eclogae Geol. Helv.* 94, 265–287.
- ALLENBACH, R.P. (in press): Spatial patterns of Mesozoic facies relationships and the age of the upper Rhinegraben Lineament – a review. *International Journal of Earth Sciences* (in press).
- BERGER, A., LOUTRE, M.F. & DEHANT, V. 1989: Astronomical frequencies for pre-Quaternary palaeoclimate studies. *Terra Nova* 1, 474–479.
- COLOMBIÉ, C. 2002: Sédimentologie, stratigraphie séquentielle et cyclostratigraphie du Kimméridgien du Jura suisse et du Bassin vocontien (France): relations plate-forme – bassin et facteurs déterminants. *GeoFocus* 5, 198 p.
- DERCOURT, J., GAETANI, M., VRIELYNCK, B., BARRIER, E., BIJU-DUVAL, B., BRUNET, M.F., CADET, J.P., CRASQUIN, S. & SANDULESCU, M. (Eds.) 2000: *Atlas Peri-Tethys – Palaeogeographical Maps*. Paris.
- DI GIOIA, E. 2001: Etude géologique de la région de Himmelmried (Jura bâlois et soleurois, Suisse) avec analyse séquentielle dans l'Oxfordien supérieur. Unpubl. Diploma Thesis, Fribourg, 103 p.
- DUNHAM, R.J. 1962: Classification of carbonate rocks according to their depositional texture. In: *Classification of Carbonate Rocks* (Ed. by HAM, W.E.). Amer. Assoc. Petroleum Geol. Mem. 1, 108–121.
- DUPRAZ, C. 1999: Paléontologie, paléocologie et évolution des faciès récifaux de l'Oxfordien Moyen-Supérieur (Jura suisse et français). *GeoFocus* 2, 247 p.
- DUPRAZ, C. & STRASSER, A. 1999: Microbialites and micro-encrusters in shallow coral bioherms (Middle to Late Oxfordian, Swiss Jura Mountains). *Facies* 40, 101–130.
- DUPRAZ, C. & STRASSER, A. 2002: Nutritional modes in coral-microbialite reefs (Jurassic, Oxfordian, Switzerland): Evolution of trophic structure as a response to environmental change. *Palaios* 17, 449–471.
- EMBRY, A.F., III & KLOVAN, J.E. 1972: Absolute water depth limits of Late Devonian paleoecological zones. *Geol. Rundschau* 61, 672–686.
- ENOS, P. & PERKINS, R.D. 1977: Quaternary sedimentation in South Florida. *Geol. Soc. Amer. Mem.* 147, 198 p.
- FLÜGEL, E. 1982: *Microfacies Analysis of Limestones*. Springer-Verlag, 633 p.
- GARRETT, P., SMITH, D.L., WILSON, A.O. & PATRIGUIN, D. 1971: Physiography, ecology and sediments of two Bermuda patch reefs. *J. Geol.* 79, 647–668.
- GILL, G.A., 1977: Essai de regroupement des Styliques (Hexacoralliaires) d'après la morphologie des bords internes de leurs septes. *Mém. B.R.G.M.* 89, 283–295.
- GINSBURG, R.N., HARDIE, L.A., BRICKER, O.P., GARRETT, P. and WANLESS, H.R., 1977: Exposure index: a quantitative approach to defining position within the tidal zone. In: *Sedimentation on the Modern Carbonate Tidal Flats on Northwest Andros Island, Bahamas* (Ed. by HARDIE, L.A.). Johns Hopkins Univ. Press, Baltimore, 7–11.
- GRADSTEIN, F.M., AGTERBERG, F.P., OGG, J.G., HARDENBOL, J., VAN VEEN, P., THIERRY, J. & HUANG, Z. 1995: A Triassic, Jurassic and Cretaceous time scale. In: *Geochronology, Time Scales and Global Stratigraphic Correlation* (Ed. by BERGGREN, W.A., KENT, D.V., AUBRY, M.P. & HARDENBOL, J.). Soc. Econ. Paleont. Mineral. Spec. Publ. 54, 95–126.
- GYGI, R.A. 1969: Zur Stratigraphie der Oxford-Stufe (oberes Jura-System) der Nordschweiz und des süddeutschen Grenzgebietes. *Beitr. Geol. Karte Schweiz N.F.* 136, 123 p.
- GYGI, R.A. 1995: Datierung von Seichtwassersedimenten des Späten Jura in der Nordwestschweiz mit Ammoniten. *Eclogae Geol. Helv.* 88, 1–58.
- GYGI, R.A. 2000: Integrated stratigraphy of the Oxfordian and Kimmeridgian (Late Jurassic) in northern Switzerland and adjacent southern Germany. *Mem. Swiss Acad. Sci.* 104, 152 p.
- GYGI, R.A., COE, A.L. & VAIL, P.R. 1998: Sequence stratigraphy of the Oxfordian and Kimmeridgian stages (Late Jurassic) in northern Switzerland. In: *Mesozoic and Cenozoic Sequence Stratigraphy of European Basins* (Ed. by DE GRACIANSKY, P.-C., HARDENBOL, J., JACQUIN, T. & VAIL, P.R.). Soc. Econ. Paleont. Mineral. Spec. Publ. 60, 527–544.
- GYGI, R.A. & PERSOZ, F. 1986: Mineralostratigraphy, litho- and biostratigraphy combined in correlation of the Oxfordian (Late Jurassic) formations of the Swiss Jura range. *Eclogae Geol. Helv.* 79, 385–454.
- HARDENBOL, J., THIERRY, J., FARLEY, M.B., JACQUIN, T., DE GRACIANSKY, P.-C. & VAIL, P.R. 1998: Charts. In: *Mesozoic and Cenozoic Sequence Stratigraphy of European Basins* (Ed. by DE GRACIANSKY, P.-C., HARDENBOL, J., JACQUIN, T. & VAIL, P.R.). Soc. Econ. Paleont. Mineral. Spec. Publ. 60.
- HUG, W.A. 2003: Sequenzielle Faziesentwicklung der Karbonatplattform des Schweizer Jura im späten Oxford und frühesten Kimmeridge. *GeoFocus* 7, 156p.
- JAMES, N.P. & BOURQUE, P.-A. 1992: Reefs and mounds. In: *Facies Models: Response to Sea Level Change* (Ed. by WALKER, R.G. AND JAMES, N.P.). Geol. Assoc. Canada, 323–347.
- JAMES, N.P. & GINSBURG, R.N. 1979: The seaward margin of Belize barrier and atoll reefs. *Int. Assoc. Sedimentol. Spec. Publ.* 3, 191 p.

- JORDAN, C.F.Jr. 1973. Carbonate facies and sedimentation of patch reefs off Bermuda. *Amer. Assoc. Petrol. Geol. Bull.* 57, 42–54.
- LAUBSCHER, H. 1995: Neues zur Grenzzone Tafeljura–Faltenjura (Gebiet von Ziefen–Reigoldswil, Baselbieter Jura). *Eclogae Geol. Helv.* 88, 219–234.
- NEUMANN, A.C., GEBELEIN, C.D. & SCOFFIN, T.P. 1970: The composition, structure, and erodability of subtidal mats, Abaco, Bahamas. *J. Sed. Petrol.* 40, 274–297.
- PITTET, B. 1996: Contrôles climatiques, eustatiques et tectoniques sur des systèmes mixtes carbonates-siliciclastiques de plate-forme: exemples de l'Oxfordien (Jura suisse, Normandie, Espagne). Unpubl. PhD Thesis, Fribourg, 258 p.
- PITTET, B. & STRASSER, A. 1998: Long-distance correlations by sequence stratigraphy and cyclostratigraphy: examples and implications (Oxfordian from the Swiss Jura, Spain, and Normandy). *Geol. Rundschau* 86, 852–874.
- PRATT, B.R., JAMES, N.P. and COWAN, C.A., 1992. Peritidal carbonates. In: *Facies Models: Response to Sea Level Change* (Ed. by WALKER, R.G. AND JAMES, N.P.). *Geol. Assoc. Canada*, 303–322.
- PURSER, B.H. (Ed.) 1973: *The Persian Gulf*. Springer-Verlag, 471 p.
- RAUBER, G. 2001: Géologie de la région de Bärschwil-Grindel (Jura soleurois, Suisse) avec analyse détaillée de l'Oxfordien supérieur. Unpubl. Diploma Thesis, Fribourg, 109 p.
- REITNER, J., NEUWEILER, F., FLAJS, G., VIGENER, M., KEUPP, H., MEISCHNER, D., PAUL, J., WARNKE, K., WELLER, H., DINGLE, P., HENSEN, C., SCHÄFER, P., GAUTRET, P., LEINFELDER, R.R., HÜSSNER, H. & KAUFMANN, B. 1995: Mud mounds – a polygenetic spectrum of fine-grained carbonate buildups. *Facies* 32, 1–69.
- SHINN, E.A. 1983: Tidal flat environment. In: *Carbonate Depositional Environments* (Ed. by SCHOLLE, P.A., BEBOUT, D.G. & MOORE, C.H.). *Amer. Assoc. Petroleum Geol. Mem.* 33, 171–210.
- SHINN, E.A., LLOYD, R.M. and GINSBURG, R.N. 1969: Anatomy of a modern carbonate tidal-flat, Andros Island, Bahamas. *J. Sed. Petrol.* 39, 1202–1228.
- SCHREIBER, B.C. 1986: Arid shorelines and evaporites. In: *Sedimentary Environments and Facies* (2nd ed.) (Ed. by READING, H.G.). Blackwell, 189–228.
- SCHWEIGERT, G. 1995: *Amoebopeltoceras* n.g., eine neue Ammonitengattung aus dem Oberjura (Ober-Oxfordium bis Unter-Kimmeridgium) von Südwestdeutschland und Spanien. *Stuttgarter Beitr. Naturkunde Ser. B* 227, 1–12.
- SCOFFIN, T.P. 1970: The trapping and binding of subtidal carbonate sediments by marine vegetation in Bimini lagoon, Bahamas. *J. Sed. Petrol.* 40, 249–273.
- SCOFFIN, T.P. 1987: *Carbonate Sediments and Rocks*. Blackie, 274 p.
- STEINMANN, G. 1880: Die Mumien des Hauptrogensteins. *N. Jb. Min. Geol. Paläont.* 1, 151–154.
- STRASSER, A. 1986: Ooids in Purbeck limestones (lowermost Cretaceous) of the Swiss and French Jura. *Sedimentology* 33, 711–727.
- STRASSER, A., 1991: Lagoonal-peritidal sequences in carbonate environments: autocyclic and allocyclic processes. In: *Cycles and Events in Stratigraphy* (Ed. by EINSELE, G., RICKEN, W. & SEILACHER, A.). Springer-Verlag, 709–721.
- STRASSER, A. & HILLGÄRTNER, H. 1998: High-frequency sea-level fluctuations recorded on a shallow carbonate platform (Berriasian and Lower Valanginian of Mount Salève, French Jura). *Eclogae Geol. Helv.* 91, 375–390.
- STRASSER, A., PITTET, B., HILLGÄRTNER, H. & PASQUIER, J.-B. 1999: Depositional sequences in shallow carbonate-dominated sedimentary systems: concepts for a high-resolution analysis. *Sed. Geol.* 128, 201–221.
- STRASSER, A., HILLGÄRTNER, H., HUG, W., AND PITTET, B. 2000: Third-order depositional sequences reflecting Milankovitch cyclicity. *Terra Nova* 12, 303–311.
- STRASSER, A., HILLGÄRTNER, H. & PASQUIER, J.-B. 2003: Cyclostratigraphic timing of sedimentary processes: an example from the Berriasian of the Swiss and French Jura Mountains. *Soc. Econ. Paleont. Mineral. Spec. Publ.* (in print).
- TUCKER, M.E. 1985: Shallow-marine carbonate facies and facies models. In: *Sedimentology: Recent Developments and Applied Aspects* (Ed. by BRENCHEY, P.J. & WILLIAMS, B.P.J.). *Geol. Soc. (London) Spec. Publ.* 18, 311–338.
- TUCKER, M.E. & WRIGHT, V.P. 1990: *Carbonate Sedimentology*. Blackwell, 482 p.
- VAIL, P.R., AUDEMARD, F., BOWMAN, S.A., EISNER, P.N. & PEREZ-CRUZ, C. 1991: The stratigraphic signatures of tectonics, eustasy and sedimentology – an overview. In: *Cycles and Events in Stratigraphy* (Ed. by EINSELE, G., RICKEN, W. & SEILACHER, A.). Springer-Verlag, 617–659.
- WHEELER, H.E. 1964: Baselevel, lithosphere surface, and time stratigraphy. *Geol. Soc. Amer. Bull.* 75, 599–610.
- ZIEGLER, P.A. 1956: Geologische Beschreibung des Blattes Courtelary (Bern-Jura) und zur Stratigraphie des Séquanien im zentralen Schweizer Jura. *Beitr. Geol. Karte Schweiz N.F.* 102, 101 p.
- ZIEGLER, P.A. 1988: Evolution of the Arctic – North Atlantic and the Western Tethys. *Amer. Ass. Petroleum Geol. Mem.* 43, 198 p.

Manuscript received December 20, 2002

Revision accepted August 9, 2003